

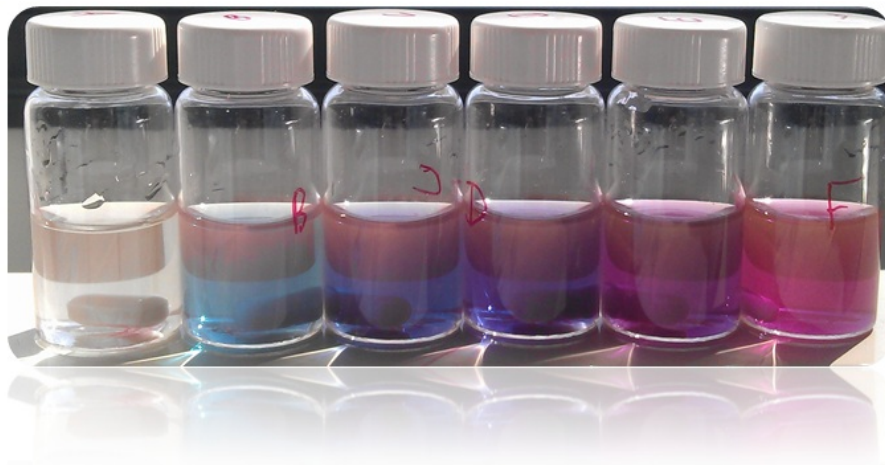


Universiteit Utrecht

MSc THESIS

PART A

Dye functionalised silica coated gold nanoparticles to study localized surface plasmon - dye interactions



Author:
Jantina Fokkema

Supervisors:
F.T. Rabouw, MSc
R.J.A. Moes, MSc
prof. dr. D.A.M. Vanmaekelbergh

August 9, 2014

Abstract

Gold nanoparticles are the most stable known metal nanoparticles. These particles exhibit very unique optical properties caused by plasmonic effects. A consequence of these plasmonic effects is the possibility of coupling between a gold particle and an emitter. In a recent paper by Reineck et al., titled "*Distance and Wavelength Dependent Quenching of Molecular Fluorescence by Au@SiO₂ Core-Shell Nanoparticles*", this coupling was studied for different dyes as a function of the gold-dye spacing. Gold nanoparticles with a radius of 12.7 nm were used and spacing was induced by a silica shell. A theoretical model was presented in the paper that predicts the obtained results very well which is a great achievement. However, experiments were only performed for small gold nanoparticles and only quenching of the dye emission was observed. For bigger gold nanoparticles (> 50 nm) enhancement of dye emission is possible which is much more interesting to study since plasmon-enhanced luminescence is promising in a lot of fields. The goal of this research is to extend the work by Reineck et al. by performing similar experiments with bigger particles to study enhancement of the dye emission.

This research started with a two step synthesis of the gold nanoparticles needed for the experiments. In the first step, small gold seeds with diameters close to 15 nm were synthesized via the citrate reduction method. Subsequently, these seeds were grown larger by using hydroquinone as a reductor to selectively reduce additional gold salt onto the surface of the existing nanocrystals. By tuning the number of seeds added in this step, it was possible to synthesize gold nanoparticles with diameters from 50 to 200 nm. Transmission electron microscopy and absorption measurements were used to characterize the samples. It was clearly observed that absorption shifts to longer wavelengths with increasing gold diameters. Furthermore, peak broadening and an increase in scattering was observed with increasing particle size.

To obtain stable dispersions of the particles in ethanol, particles were capped with polyvinylpyrrolidone. These particles were coated with uniform layers of silica via an adjusted Stöber process. To do so, ammonia was added to the gold nanoparticle solution first. Small volumes of tetraethylorthosilicate were added next for the shells to grow. After some optimization, a procedure was developed to reproducibly coat the gold particles with uniform layers of silica.

After silica coating the outer surface of the particles was functionalised with (3-aminopropyl) triethoxysilane introducing -NH₂ groups at the surface. These -NH₂ groups were used to bind the activated ATTO700 dye. Photoluminescence decay measurements showed that there was coupling between the dye molecules attached to the silica coated gold nanoparticles and the gold particles. This was indicated by the presence of a second, much faster decay path that was only observed in the presence of the gold nanoparticles. In order to learn more about the observed gold-dye coupling a comprehensive study is necessary. It would be interesting for example to study the distance dependence of this coupling for bigger nanoparticles and to study this coupling for different sizes of gold nanoparticles. This should be achievable since a reproducible procedure to synthesize the samples is demonstrated in this thesis.

Contents

1	Introduction	3
2	Theoretical background	5
2.1	Plasmonic effects for gold nanoparticles: unique optical properties	5
2.2	Distance and wavelength dependent quenching	7
2.3	An adjusted Stöber process for Si shell growth	8
3	Synthesis of PVP stabilized gold nanoparticles (50-200 nm)	10
3.1	Synthesis of gold seeds	11
3.2	Growth of the gold seeds	12
3.3	Growth of gold seeds on a bigger scale	14
3.4	Obtaining more spherical gold particles	15
3.5	Transfer of the gold nanoparticles to ethanol	16
4	Silica coating of the PVP capped gold nanoparticles	17
4.1	Results: Shell growth(1)	17
4.2	Shell growth, secondary nucleation and PVP concentration	20
5	APTES functionalisation of the silica coated gold nanoparticles	22
6	Dye attachment and gold-dye coupling	24
6.1	Gold-dye coupling: theoretical calculations	24
6.1.1	Atto700 stock solution - Absorption measurements	26
6.2	Dye binding 1	26
6.2.1	TEM measurements	27
6.3	Dye binding 2	27
6.3.1	Emission measurements	28
6.4	Dye binding 3	29
6.4.1	Emission measurements	29
7	Conclusion	33
8	Outlook	35
	Bibliography	39
	Appendices	41
A:	Chemicals	41
B:	ATTO700 dye	42
C:	Calculation of extinction for spherical gold nanoparticles	43

Chapter 1

Introduction

Gold nanoparticles have been utilized for centuries because of their unique properties. One of the most famous examples demonstrating these unique properties is the Lycurgus cup manufactured in the 4th century A.D. by the Romans [1]. When viewed in reflected light such as daylight the cup appears green. However, when the cup is illuminated from the inside it glows ruby as shown in figure 1.1a. The cup is made of ruby glass which was one of the first optical metamaterials. The crucial ingredients responsible for the extraordinary behaviour are tiny gold droplets, typically 5 - 60 nm in size.

Another impressive example for which the unique optical properties of gold nanoparticles are used are gothic stained windows. Combinations of gold and silver nanoparticles are used to obtain the bright colors in the windows [2]. One of the windows of the Notre-Dame de Paris is depicted in figure 1.1b showing the variation in colors that can be achieved.

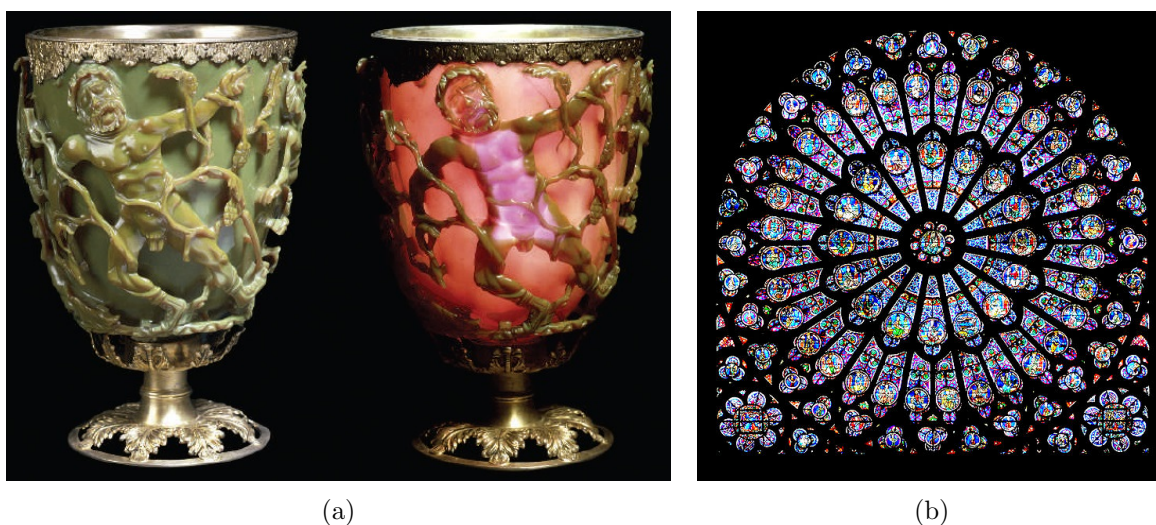


Figure 1.1: In (a) the Lycurgus cup under reflection (left) and transmittance (right). In (b) the Gothic stained glass rose window of the Notre-Dame de Paris. The wide variety of colors is due to metal nanoparticles.

Gold nanoparticles are the most stable known metal nanoparticles. These nanoparticles present fascinating aspects such as the behavior of the individual particles, size-related electronic, magnetic and optical properties and their applications in catalysis and biology. Their promises are in these fields as well as in the bottom-up approach of nanotechnology and they will be key

materials and building blocks in the 21st century [3]. The synthesis of spherical gold nanoparticles has been studied extensively in the past. Previous studies have shown that spherical gold nanoparticles can be synthesized with high monodispersity and reproducibility very easily. Back in 1857 Faraday already reported the formation of deep-red solutions of colloidal gold by reduction of an aqueous solution of chloroaurate (AuCl_4^-) using phosphorus (CS_2). This synthesis is in principle very comparable to the one described in this thesis.

The optical properties of gold particles are determined by so-called plasmonic effects, described in more detail in section 2.1. A consequence of these plasmonic effects is the possibility of coupling between a gold particle and an emitter. This coupling is also observed for other plasmonic materials as well and results in quenching or enhancement of the emitter. The amount of quenching or enhancement in such a system is determined by the spacing between the two. Typically for small particles (< 10 nm) quenching of the emission is observed whereas at bigger diameters (> 50 nm) enhancement is possible [4].

In a recent paper by Reineck et al., titled "*Distance and Wavelength Dependent Quenching of Molecular Fluorescence by Au@SiO₂ Core-Shell Nanoparticles*", such a system was studied. Coupling between gold nanoparticles with a radius of 12.7 nm and different dyes was studied as a function of spacing between the two. This spacing was induced by the presence of a silica shell between the gold nanoparticles and the dyes attached to the outer surface of the spheres. A theoretical model was presented in the paper that predicts this results very well which was a great achievement. However, experiments were only performed for small gold nanoparticles so only quenching of the dye emission is observed. However, it would be much more interesting to study the enhancement of dye emission because plasmon-enhanced luminescence is promising in a lot of fields.

The goal of this research is to perform experiments similar to the experiments performed by Reineck et al. for bigger gold nanoparticles (> 50 nm). For these particles also enhancement of the dye emission should be observable. This would enable us to test whether the theoretical models presented in the paper also holds for plasmon-enhanced luminescence.

Chapter 2

Theoretical background

2.1 Plasmonic effects for gold nanoparticles: unique optical properties

A surface plasmon is a coherent oscillation of the surface conduction electrons of a metal which can be excited by electromagnetic radiation. These surface plasmons can run over interfaces between materials having opposite signs of the dielectric function such as a metal-air or a metal-dielectric interface. Here the coherent oscillation of electrons creates an electromagnetic field across the surface. Plasmon polaritons, depicted in figure 2.1a, can propagate in both the x- and y- direction along the metal-dielectric interface for distances in the order of tens to hundreds of microns. For a surface plasmon wave running over a gold-water interface this value corresponds to 3 microns for a wave with a free space wavelength of 630 nm and 24 microns at 850 nm [5]. In the z-direction the plasmon decays evanescently with $1/e$ decay lengths on the order of 200 nm [6].

When particles much smaller than the incident wavelength of light are excited, a plasmon that oscillates locally around the nanoparticle as depicted in figure 2.1b is obtained. The frequency that can be used to excite such an oscillation or localized surface plasmon is known as the localized surface plasmon resonance (LSPR).

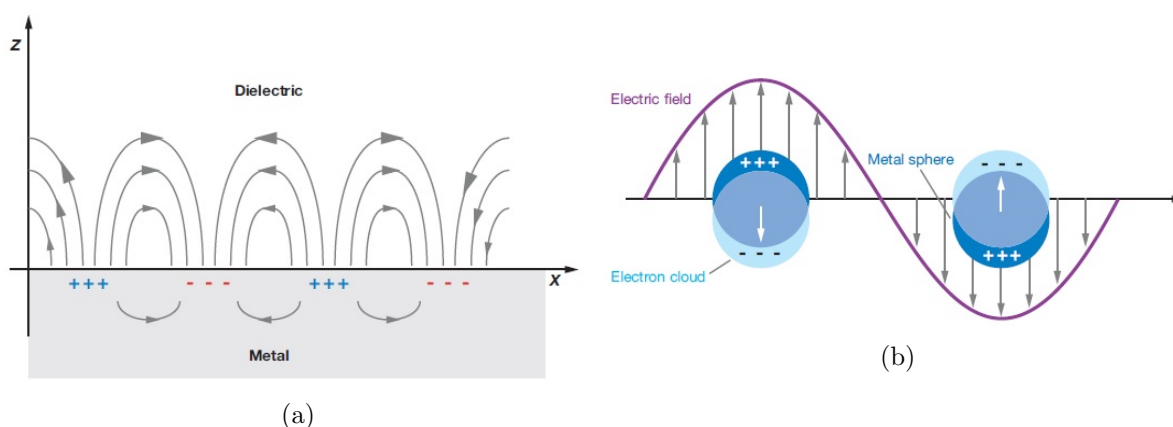


Figure 2.1: In (a) a schematic depiction of a surface plasmon polariton (or propagating plasmon). In (b) a schematic depiction of a localized surface plasmon found when particles much smaller than the incident wavelength of light are excited.

For metal nanoparticles, such as the gold nanoparticles used in the experiments, most of the optical properties originate from the presence of localized surface plasmons. When these nanoparticles are exposed to light, a number of processes can occur as depicted in figure 2.2 [7]:

- the light can be absorbed;
- the light can be scattered at the same frequency as the incoming light (Mie/Rayleigh scattering);
- the absorbed light can be re-emitted (i.e. fluorescence);
- the local electromagnetic field on the incoming light can be enhanced, thereby enhancing any spectroscopic signals from the molecules at the material surface, that is, surface enhanced spectroscopy, such as surface enhance Raman spectroscopy (SERS).

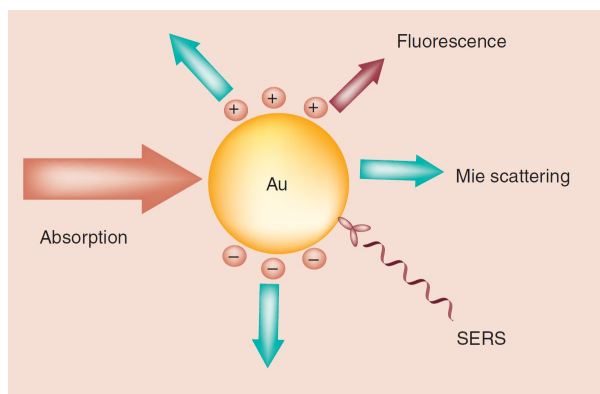


Figure 2.2: Important optical processes resulting from the interaction of light with a gold nanoparticle which can be: absorption of light, Mie scattering, surface-enhanced luminescence and surface-enhanced Raman scattering from absorbed molecules.

These four processes can be strongly enhanced by the presence of a LSPR. Since the frequency of the LSPR strongly depends on particle size and shape, optical properties also become size and shape dependent. This makes it possible to tune the optical properties by changing size and/or particle shape. For spherical gold nanoparticles LSPR are typically found in the visible region where the exact position depends on the size of the spheres and the refractive index of the medium in which the particles are dispersed. The presence of a LSPR results in extremely high absorption and scattering of spherical gold. Gold nanoparticles with a radius of 40 nm can be detected easily by eye down to a particles concentration of 10^{-14} M. For gold nanoparticles of 60 nm, scattering is 10^5 times stronger than the emission of a fluorescent molecule.

2.2 Distance and wavelength dependent quenching

As mentioned in the introduction, part of the experimental work described in this thesis is based on work done by Reineck *et al.* [8]. A short summary mentioning the key points of this paper is given in the coming section.

In the article the coupling of the near-field of a gold nanoparticle with nearby excited states of a fluorescent dye molecule is investigated where coupling is a results of the plasmonic properties of gold. To investigate this coupling, gold nanoparticles with a diameter of 12.7 ± 0.3 nm were synthesized. These nanoparticles were coated with a silica shell which was functionalised with (3-aminopropyl)triethoxysilane. After functionalisation a dye was bound to the surface of the particles as depicted schematically in figure 2.3a. Here the silica shell acts as a rigid spacer between the gold core and the dye. The spacing, d , was varied from 4 to 43 nm and coupling for 4 different dyes was studied.

Besides the experimental work, a theoretical model to interpreted the results is also presented in the article. Using this theoretical model the relative fluorescence intensity I/I_0 and the relative fluorescence lifetime τ/τ^0 are calculated as a function of the nanoparticle-dye separation d . Here I_0 and τ_0 correspond to the fluorescence intensity and fluorescence lifetime of the dye attached to a silica sphere in the absence of a gold core. Calculations were performed for a normal and a tangential orientation of the dye. These calculations were averaged which results in a theory average to which the experimental results are compared.

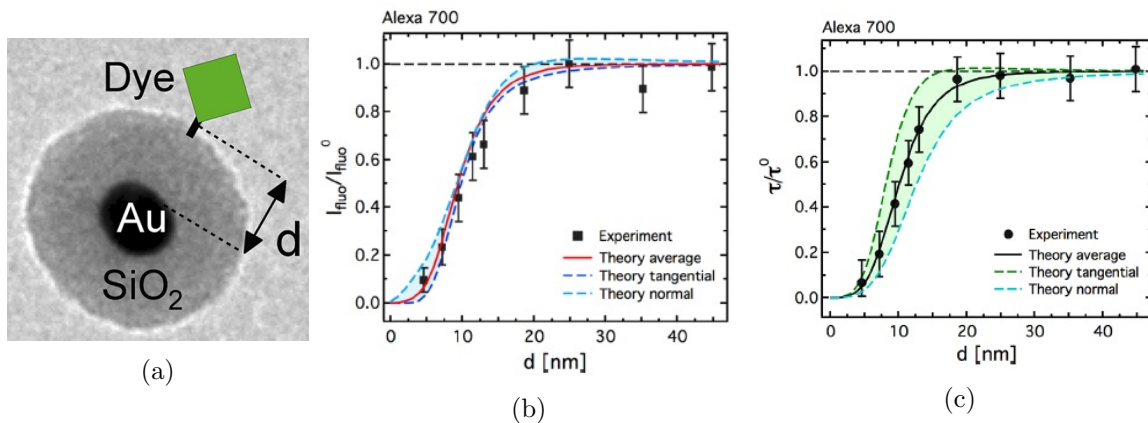


Figure 2.3: In (a) the system studied showing the silica spacer with thickness d with a dye bound to the surface. In (b) experimental and theoretical results for the relative fluorescence intensity as a function of the nanoparticle-dye separation d for the Alexa700 dye. In (c) relative fluorescence lifetime τ/τ^0 as a function of distance d between dye and gold nanoparticle. τ^0 is the fluorescence lifetime of the dye molecule bound to a silica nanoparticle, which is slightly shorter than the lifetime of the free dye in solution.

Results for both experimental and theoretical work for the Alexa 700 dye are depicted in figure 2.3b and c. From figure b and c it can be seen that there is a regime going from nearly complete quenching, at small values of d , to a regime where the presence of the gold core becomes negligible, d values bigger than 20 nm. It can be seen that the theoretical model presented in the paper quantitatively predicts the observed quenching of fluorescence and shortening of the fluorescence lifetime.

In the growth process, a diluted solution tetraethylorthosilicate (TEOS) in ethanol and a solution containing ammonia, water and ethanol are added over time to the seed suspension in ethanol under constant stirring as depicted in figure 2.5. Reaction conditions are chosen in such a way that silica is formed on top of the seeds without any secondary nucleation. The final size of the spheres is now determined by the initial diameter and concentration of the seeds and the total amount of tetraethylorthosilicate added during the process.

Reaction conditions such as pH, TEOS concentration and ionic strength are of big importance in this process. As depicted in figure 2.6 there is a competition between new nucleation of silica and silica deposition on existing particles. The balance between the two is affected by those reaction conditions. By finding the right pH for the reaction and the right addition speed of TEOS the concentration of the reaction intermediates can be affected. The concentration of reaction intermediates should be high enough for the reaction to proceed in an acceptable time range but should not be so high that nucleation occurs. It is also possible to decrease the distance that intermediates have to travel before finding a seed particle, the so called diffusion length. This can be achieved by increasing the concentration of seeds within the reaction mixture and increases the probability of silica deposition on the existing particles.

In an ideal situation reaction conditions are chosen in such a way that all silica formed during the reaction is deposited on the existing particles without the formation of any new nucleus. This would make it very easy to tune particles size (shell thickness) simply by changing the total amount of TEOS added during the reaction.

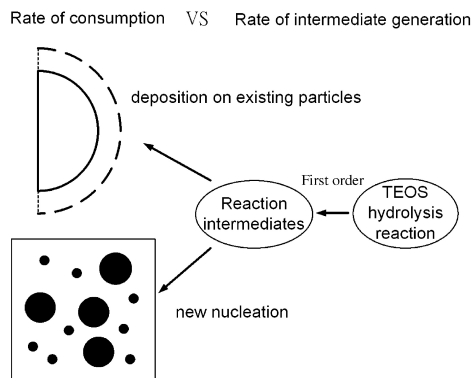


Figure 2.6: Schematic graph of the generation and consumption of intermediate for particle growth [11].

Since we are interested in the coating of gold nanoparticles with layers of silica, we are interested in using gold nanoparticles as seeds. Successful coating of gold nanoparticles by doing this is demonstrated in various papers [12, 13, 14, 15].

Chapter 3

Synthesis of PVP stabilized gold nanoparticles (50-200 nm)

In this chapter a two step synthesis of gold nanoparticles with diameters from 50 to 200 nm is described. To obtain stable dispersion of the particles in ethanol, particles are capped with PVP. An overview of the reaction process is included in figure 3.1.

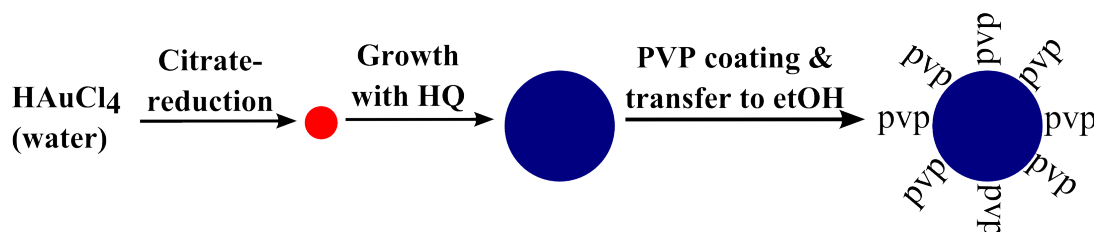


Figure 3.1: Overview of the reaction: gold seeds are prepared via the citrate reduction, extra gold is reduced onto the existing seeds using hydroquinone as a reductor to obtain particles with diameters ranging from 50 to 200 nm. These particles are coated with PVP and transferred to ethanol.

Gold nanoparticles are synthesized in two separated steps as described by Perrault and Chan [16]. In the first step gold seeds are prepared using the well known citrate reduction. This results in spherical gold nanoparticles with a diameter of approximately 15 nm which are citrate stabilized and therefore carry a negative surface charge.

In the second step extra gold is reduced onto the surface of the seeds to obtain bigger nanoparticles. For this reaction hydroquinone is used as a reductor. Since there is a small difference in reduction potential between reducing gold chloride in the presence of metal clusters and reducing isolated Au^{I} to Au^0 it is possible to deposit gold selectively onto the surface of the seeds. Hydroquinone is chosen as the reductor in this step because for this reductor only the deposition of gold onto the surface of the seeds is a spontaneous process at room temperature. The reaction scheme is depicted in figure 3.2. During the growth of the seeds, also some sodiumcitrate dihydrate is added for stabilisation of the particles.

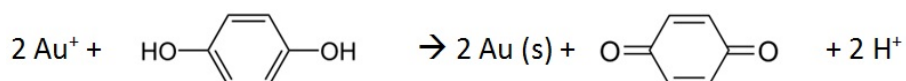


Figure 3.2: Reaction for the reduction of gold salt into solid gold using hydroquinone as a reductor.

It is possible to tune the final size of the nanoparticles simply by varying the number of seeds added in this step at constant gold (Au^+) concentration. By doing this, particles with diameters from 50 to 200 nm can be synthesized. The biggest gold nanoparticles are obtained when the minimum number of seeds is used. By increasing the number of seeds, the average particle size is decreased.

To coat the prepared gold nanoparticles with silica it is necessary to transfer the particles to ethanol. However, the citrate stabilized particles tend to cluster when in ethanol. To solve this problem, the particles are capped with poly(vinylpyrrolidone) (PVP) as described by Graf *et al.* [15]. PVP is an amphiphilic, nonionic polymer depicted in figure 3.3 that adsorbs onto a broad range of different materials such as metals, in this case gold. This polymer stabilizes colloidal particles in water and many non-aqueous solutions such as ethanol and serves as a coupling agent when particles are coated with silica. For this synthesis PVP10 is used, which corresponds to PVP with an average weight of 10 kg per mol.

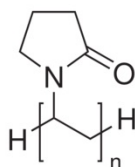


Figure 3.3: Structural formula of Poly(vinylpyrrolidone) or PVP where n can be any positive number. The gold nanoparticles are coated with this polymer to obtain stable dispersions in ethanol.

3.1 Synthesis of gold seeds

In this section the first reaction step is described. The goal is to synthesize gold seed with diameters close to 15 nm via the citrate reduction.

Before the actual reaction was started, a (*cit*)-solution was freshly prepared every day by transferring 0.10 g sodiumcitrate dihydrate and 10 mL water to a vial. An (*Au*)-solution was prepared by transferring 0.10 g chloroauric acid and 10 mL water to a vial. This solution has to be stored in a dark place and is centrifuged 10 min at 3500 rpm before usage to remove aggregates.

For the actual synthesis, 30 mL water and 300 μL (*Au*)-solution were transferred to a 250 mL beaker. The solution was stirred and heated until the boiling point was reached. When the solution started to boil, 900 μL (*cit*)-solution was added. The solution was boiled for another 10 minutes. Particle formation was indicated during the first couple of minutes of the reaction by a color transition of the solution. As soon as no color change was observed anymore, the solution was cooled down to room temperature. In a successful synthesis, the final solution had a deep red color.

Representative TEM pictures of one of the seed solutions are shown in figure 3.4. It can be seen that the seeds are nearly spherical and very uniform in size. The average diameter determined from the picture is 16 nm. All other seeds prepared have an average diameter close to 16 nm. Only samples showing the same uniformity in size and shape were used for further experiments.

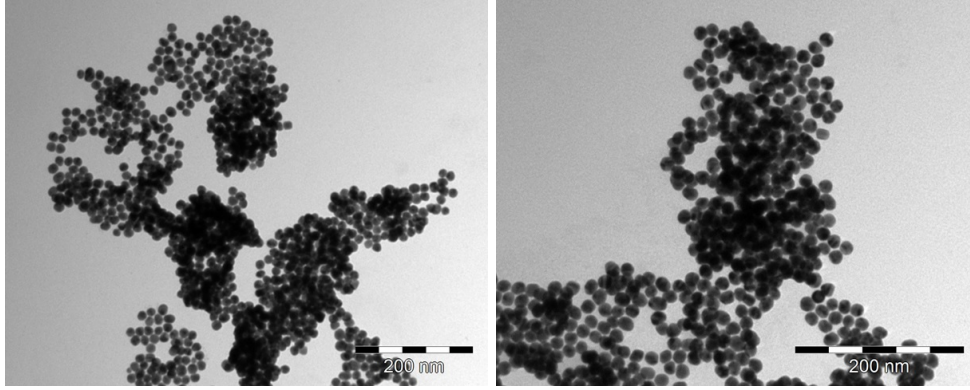


Figure 3.4: TEM pictures of gold seeds prepared via the citrate reduction.

3.2 Growth of the gold seeds

As a second step, the in section 3.1 prepared seeds are grown bigger. This can be achieved by the reduction of extra gold chloride on top of the existing seeds. The goal is to obtain spherical particles with diameters from 50 to 200 nm.

Before growth was started, a (*HQ*)-solution was prepared fresh every day by transferring 0.33 g hydroquinone and 10 mL water to a flask. The (*cit*)-solution and (*Au*)-solution described in paragraph 3.1 were also used in this reaction step.

For the actual growth of the seeds, 9.4 - 9.8 mL water (depending on the balance of water added with seeds) and 10 μL - 400 μL (depending of the desired size) of seed solution were transferred to a flask. This solution was stirred rapidly. 100 μL (*Au*)-solution was added to the solution. After at least one minute of stirring, 22 μL (*cit*)-solution and 100 μL (*HQ*)-solution were also added. After addition of the (*HQ*)-solution a change in color was observed immediately indicating the growth of the seeds. Reactions were finished as soon as no change in color was observed anymore. The reaction time could take a couple of minutes depending on the final size of the particles. The color of the remaining solutions also depended on the final size of the particles.

Preparation of a gold rainbow

Gold nanoparticles with different sizes were prepared by varying the amount of seed solution used in the reactions. The volumes of seed-solution and water used in the different reactions is summarized in table 3.1.

Sample	μL seed-solution (SII)	ml water
A	8	9.8
B	100	9.7
C	200	9.6
D	300	9.5
E	400	9.4
F	500	9.3

Table 3.1: Volumes of water and gold seeds used to synthesize gold nanoparticle with different sizes. The total reaction volume was 10 mL. 100 μL (*Au*)-solution and 100 μL (*HQ*)-solution were used in all reactions.

Characterization by TEM and absorption measurements

Representative TEM pictures of samples A-D and F are shown in figure 3.5 (a) up to (e). TEM pictures of sample E are missing since no usable pictures were obtained for this sample. TEM pictures of the seeds used to synthesize samples A to F are shown in (f). It can be seen that the nanoparticle size can be tuned by varying the amount of seeds since the size is decreasing from A to F. This increase in size is a result of the increasing number of gold seeds used in every synthesis. Bigger particles become less spherical and the irregularities of the surface increase with increasing size. The TEM pictures were used to determine the average particle size.

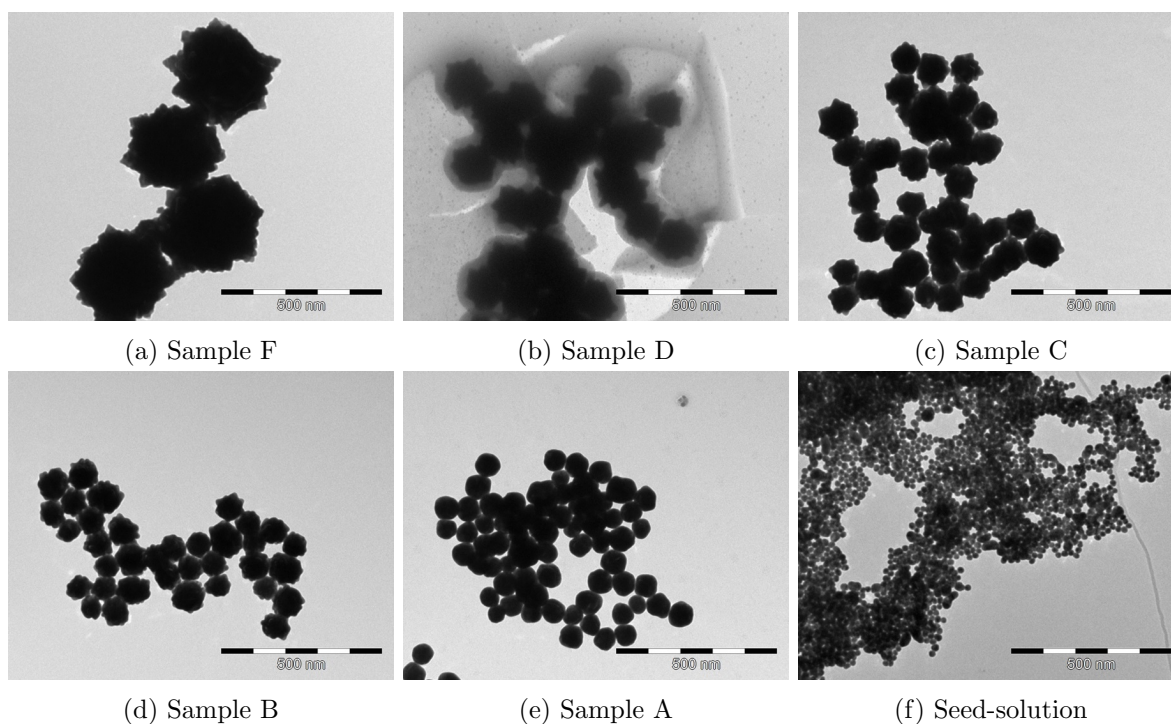


Figure 3.5: TEM pictures of gold nanoparticles with different diameters. Pictures of the seeds used to synthesize samples A-F are shown in (f).

In order to determine how the average size of the particles and the absorption (and thereby the color of the solutions) is related, normalised absorption spectra and pictures of the different solutions are shown in figure 3.6. It can be seen that the absorption shifts to longer wavelengths with increasing diameters. Also peak broadening is observed for increasing sizes which is in agreement with theory [17]. From the appearance of the solutions and the peak broadening in the absorption spectra it can be seen that the amount of scattering is strongly increasing for bigger gold particles.

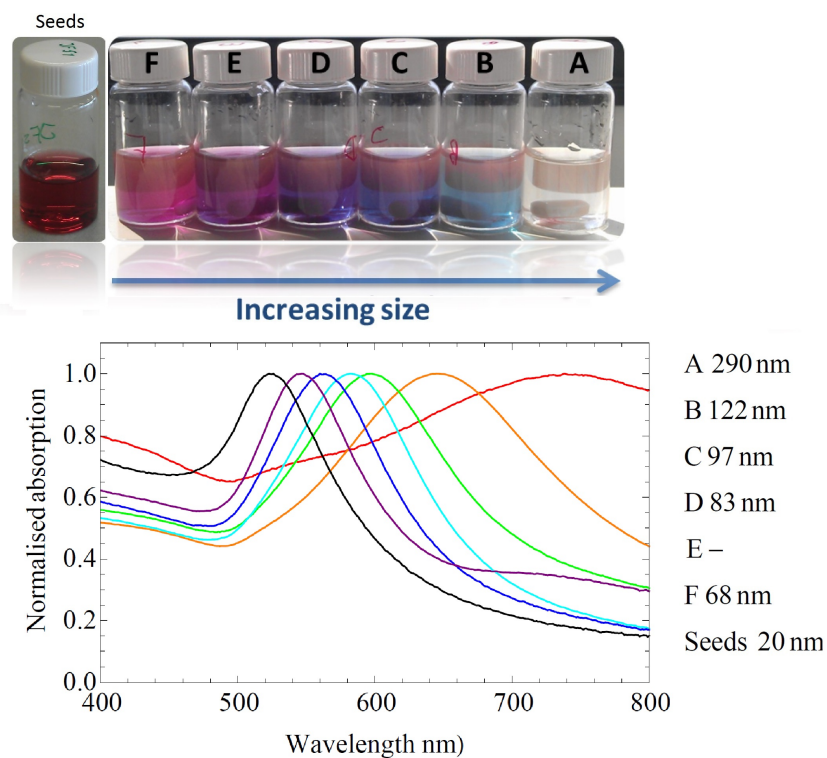


Figure 3.6: Colors of the different solutions, corresponding diameters and normalised absorption spectra. The diameters included in the legend are determined from TEM pictures.

3.3 Growth of gold seeds on a bigger scale

To obtain large numbers of gold nanoparticles the growth reaction was performed on a larger scale. To perform the reaction on a larger scale, 50 mL water and 750 μL - 4000 μL (depending of the desired size) of seed-solution were transferred to a vial. The solution was stirred rapidly. 1000 μL (*Au*)-solution was added to the solution. After at least one minute of stirring, 220 μL (*cit*)-solution and 1000 μL (*HQ*)-solution were also added. After addition of the (*HQ*)-solution a change in color was observed immediately indicating the growth of the seeds. Reactions were finished as soon as no change in color was observed anymore. Reaction times varied from several seconds up to minutes depending on the final size of the particles.

TEM measurements showed that spherical particles with different diameters could be synthesized with this method.

3.4 Obtaining more spherical gold particles

From figure 3.7 it can be seen that the surface of gold nanoparticles, synthesized using 220 μL of citrate solution and fast addition of hydroquinone solution, becomes very irregular when bigger particles are synthesized. When these particles are coated with silica, which will be described in chapter 4, also the silica surface shows these irregularities. This can be seen in figure 3.7a. In order to obtain more spherical and monodisperse particles, with a diameter around 200 nm, 2 adjustments were made in the synthesis which were tested separately.

In the first experiment, the hydroquinone solution was added dropwise. Since the progress of the reaction is determined by the presence of reductor, this should slow down the reaction. A TEM picture of the resulting particles is shown in figure 3.7b. From the picture it can be concluded that this results in clustering of the particles so this method was considered unsuccessful.

In the second experiment, the amount of citrate solution added at the beginning of the reaction was increased from 220 μL to 2000 μL . Since the particles are citrate stabilized, this might result in better stabilisation at the surface of the particles, which might lead to the formation of more spherical particles. In figure 3.7c and d TEM pictures of the resulting particles are shown. From these pictures it can be concluded that this does lead to a more spherical surface of the particles so this method is used for future experiments.

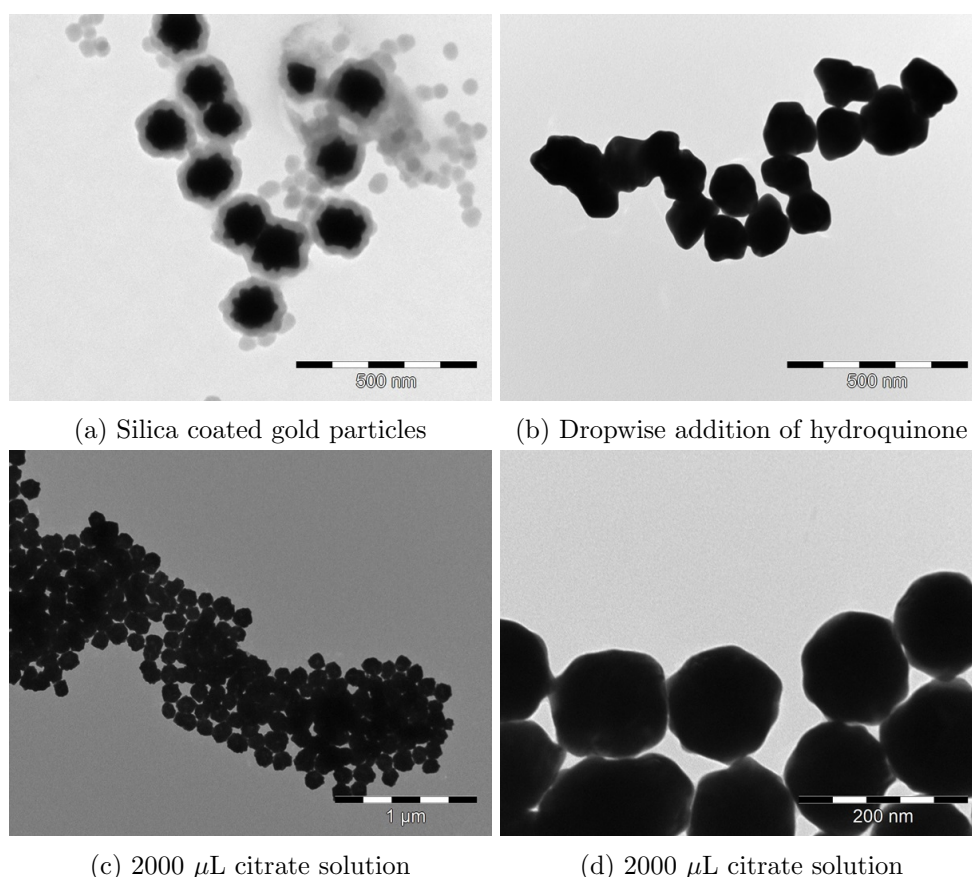


Figure 3.7: TEM pictures showing in (a) silica coated gold particles with an irregular surface, in (b) gold nanoparticles in which the hydroquinone solution was added dropwise and in (c) and (d) gold particles prepared using 2000 μL citrate solution.

3.5 Transfer of the gold nanoparticles to ethanol

Particles were coated with PVP before being transferred to ethanol. This is necessary because clustering of particles was observed when particles were transferred to ethanol in the absence of PVP.

For PVP capping, a 2.5 mM (PVP10)-solution was prepared by dissolution of 0.25 g PVP10 in 10 mL water by sonication. 5 mL of this (PVP10)-solution was added directly to 50 mL solution containing the citrate stabilized gold nanoparticles in water (see section 3.3). After 24 hours of stirring the solution was centrifuged 30 minutes at 3500 rpm. As much water as possible was removed using a pipette and the particles were resuspended in 1 mL ethanol by sonication. Washing of the particles by centrifugation was repeated three more times. Finally the particles were resuspended in 2 mL ethanol.

From TEM pictures it could be seen that the particles do not tend to cluster anymore after being transferred to ethanol after PVP capping. Stability of the gold particles also increased after PVP capping. For the nanoparticles in water without PVP irreversible clustering was observed within a couple of days indicated by a change in color of the solution. For the PVP capped particles, sedimentation was observed after storing them for a couple of hours to days depending on the size of the particles. This sedimentation was caused by gravitational forces and was observed within a shorter period of time for bigger particles. However, these particles could be resuspended easily by sonication.

Chapter 4

Silica coating of the PVP capped gold nanoparticles

The gold nanoparticles were coated with silica using an adjusted Stöber process as described in section 2.3. In this process, the PVP capped gold nanoparticles function as seeds on which the silica is deposited. The gold nanoparticles are dispersed in ethanol and after addition of ammonia, a TEOS solution in ethanol is added over time. This process is depicted schematically in figure 4.1.

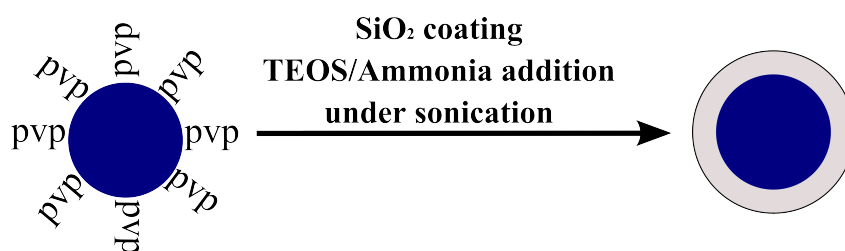


Figure 4.1: Overview of the reaction: the PVP capped gold nanoparticles are coated with a layer of silica using an adjusted Stöber process for shell growth.

4.1 Results: Shell growth(1)

A 10 vol% TEOS solution in ethanol was prepared by combining 9 mL ethanol and 1 mL TEOS to a vial.

1400 μL ethanol and 500 μL gold nanoparticle solution were transferred to a vial. 100 μL ammonium hydroxide (5 vol% in water) was added and the sample was sonicated for 30 minutes. The first TEM sample was prepared and the vial was placed in the sonicator again. Small volumes of a 10 vol% TEOS solution in ethanol were added over time, as listed in figure 4.1. Extra ammonia was added during the process and TEM samples were prepared after every addition.

After the last addition of TEOS and ammonia, the sample was sonicated for one extra hour for the reaction to finish. The sample was centrifuged for 30 minutes at 3500 rpm and particles were resuspended in 2 mL ethanol. This process was repeated 3 times before the final TEM sample was prepared.

Time (h)	
0.00	Start sonication
0.50	TEM sample (a) + 20 μL 10 vol% TEOS
2.00	TEM sample (b) + 40 μL 10 vol% TEOS
3.50	TEM sample (c) + 80 μL 10 vol% TEOS + 10 μL ammonia
5.00	TEM sample (d) + 160 μL 10 vol% TEOS + 10 μL ammonia
6.00	TEM sample (e) After washing by centrifugation TEM sample (f)

Table 4.1: Silica shell growth: 1400 μL ethanol and 500 μL gold nanoparticles were transferred to a vial after which the growth process was started under constant sonication.

In figure 4.2 TEM pictures of TEM samples (a) to (f) are shown. Sample (a) was prepared before TEOS addition so in this sample no nucleation is observed yet. In sample (b) the first nucleation of silica is observed and in sample (c) particles are coated with a thin layer of silica. The thickness of this silica layer increases when going to sample (e). However, also a lot of secondary nucleation is observed. From sample (f) it can be concluded that it is possible to remove most of these small silica particles by centrifugation. Furthermore it can be seen that the gold particles are successfully coated with a uniform layer of silica with an average thickness of 12 nm.

Experiments were also performed where the 10 vol% TEOS-solution was added using a syringe pump. Because of the small reaction volume addition with a syringe pump was not very accurate. If coating was successful results were comparable with results obtained when the TEOS-solution was added by hand. Since there was no big advantage of using the syringe pump coating was performed without it.

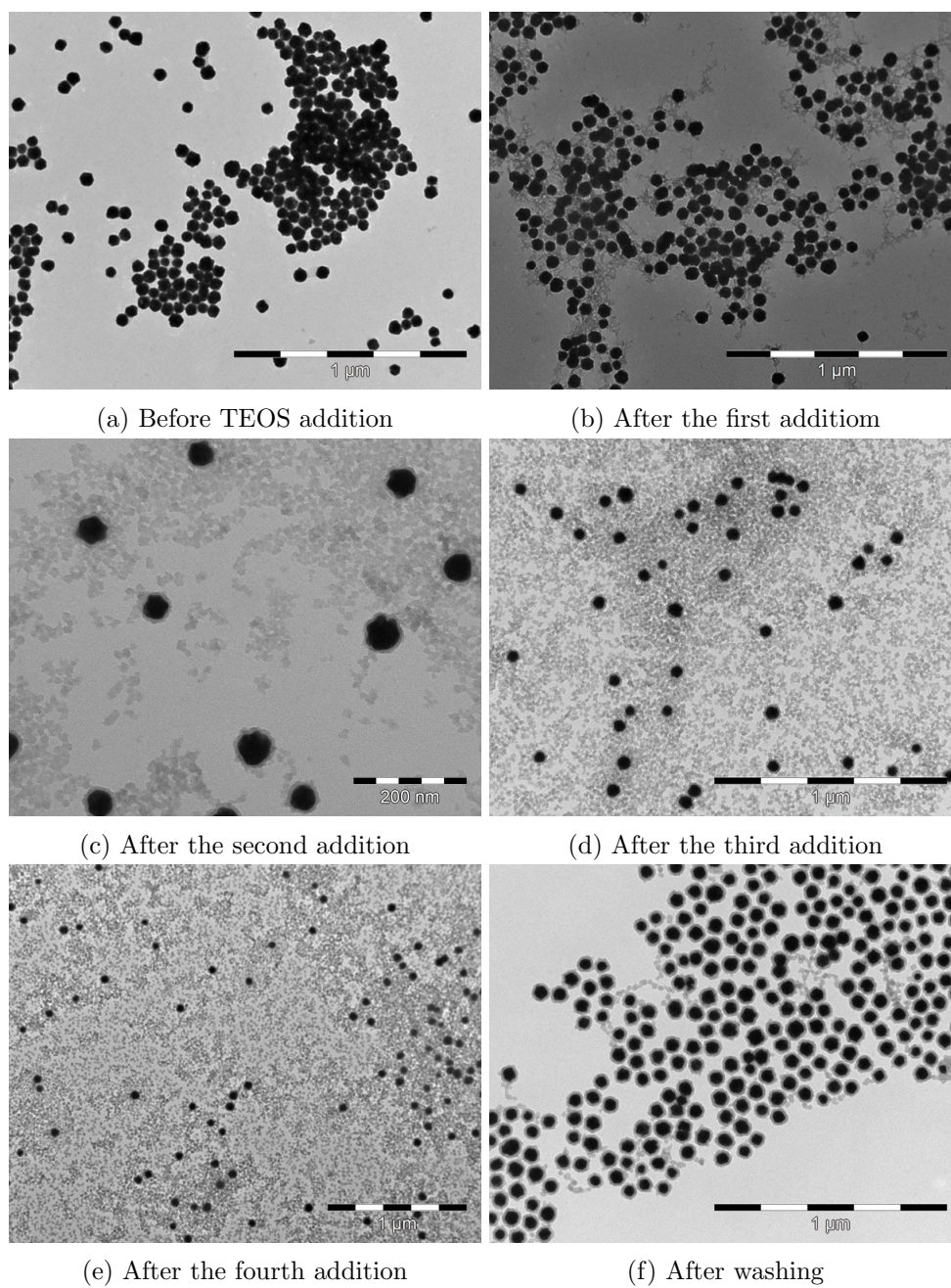


Figure 4.2: TEM pictures of samples (a)-(f) prepared in different stages of silica growth according to table 4.1. Sample (a) was prepared before TEOS was added to the solution and sample (f) was prepared after the coating and washing procedures were finished.

4.2 Shell growth, secondary nucleation and PVP concentration

For stabilisation of the prepared gold nanoparticles in ethanol an excess of PVP10 was used (see section 3.5). However, when these particles are coated with silica, a lot of secondary nucleation was observed and growth of the silica shells was a very time-consuming process. Most of the silica added during the growth process was used for secondary nucleation and not for the actual shell growth. Problems were found in the reproducibility of the shell growth and there was no control over the thickness of the shells obtained.

The thickness of the shells obtained seemed to depend strongly on the way the particles were washed after being transferred to ethanol. Particles were washed at least 3 times by centrifugation and were resuspended in ethanol before they were usable for shell growth. However, washing was a problematic and very time-consuming process.

A possible solution to overcome these problems is using smaller amounts of PVP10. According to C. Graf *et al.* an amount of 60 PVP molecules per nm^2 surface of the gold nanoparticles should be enough for stabilisation of the particles [15].

In order to investigate this, new batches of gold nanoparticles were synthesized. For stabilisation in ethanol only 100 μL of a 10 mM (PVP)-solution in water instead of 5 mL of a 2.5 mM (PVP)-solution was used. Particles were washed by centrifugation and silica shell growth started using a procedure almost identical to the one in section 4.1. 1400 μL ethanol and 500 μL gold nanoparticles were transferred to a vial and placed in the sonicator. Addition of 10 vol% TEOS and ammonia and the preparation of TEM samples was performed according to table 4.2.

Time (h)	
0	Start sonication
0.25	TEM sample (a) + 20 μL 10 vol% TEOS
1.75	+ 40 μL 10 vol% TEOS
2.50	TEM sample (b)
3.25	+ 80 μL 10 vol% TEOS + 10 μL ammonia
4.75	Start centrifugation washes
Next day	TEM sample (c)

Table 4.2: Silica shell growth for gold nanoparticles stabilized using a low PVP concentration: 1400 μL ethanol and 500 μL gold nanoparticles were transferred to a vial after which the growth process was started under constant sonication.

In figure 4.3 TEM pictures of TEM samples (a) to (c) are shown. Sample (a) was prepared before TEOS addition was started so in this sample no nucleation is observed yet. In sample (b) particles are coated with a relatively thick layer of silica already. Still some secondary nucleation of silica is observed, but the amount of nucleation is much smaller than observed in earlier experiments. From sample (c) it can be seen that it is possible to remove most of the small silica particles by centrifugation and the gold particles are successfully coated with a layer of silica with an average thickness of 29 nm.

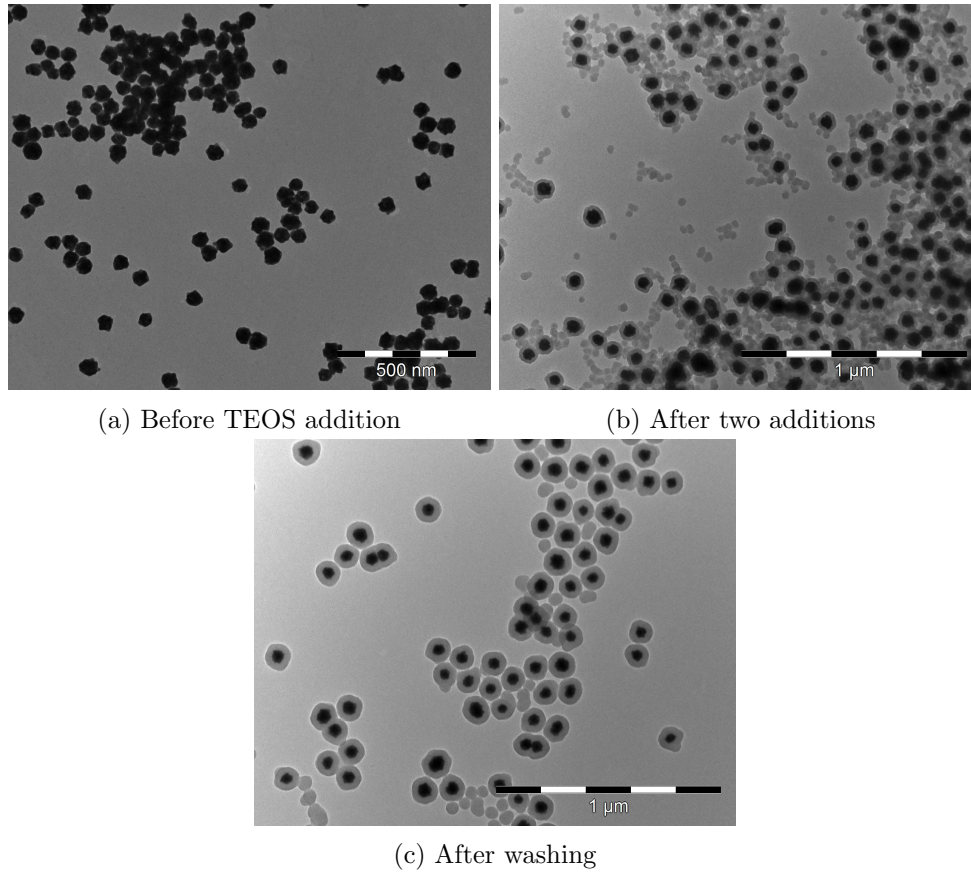


Figure 4.3: TEM pictures of samples (a)-(c) prepared in different stage of silica growth with low PVP concentration according to table 4.2. Sample (a) was prepared before TEOS was added to the solution and sample (c) was prepared after the coating and washing procedures were finished.

From this experiment it can be concluded that the silica shells formed using a lower PVP concentration are thicker after a shorter period of time, consuming less of the TEOS solution. This can be explained by a decrease in the amount of secondary nucleation of silica which makes the process much easier and faster. Further experiments have shown that control over the shell thickness obtained after coating has also increased.

Chapter 5

APTES functionalisation of the silica coated gold nanoparticles

After the gold nanoparticles were coated with a layer of silica the outer surface of the particles is functionalised with (3-aminopropyl)triethoxysilane. By functionalisation with this silane compound, -NH_2 groups are introduced at the surface of the particles as depicted schematically in figure 5.1. Functionalisation with this group is important because the -NH_2 groups at the surface can be used to bind compounds, such a dye, to the surface of the particles.

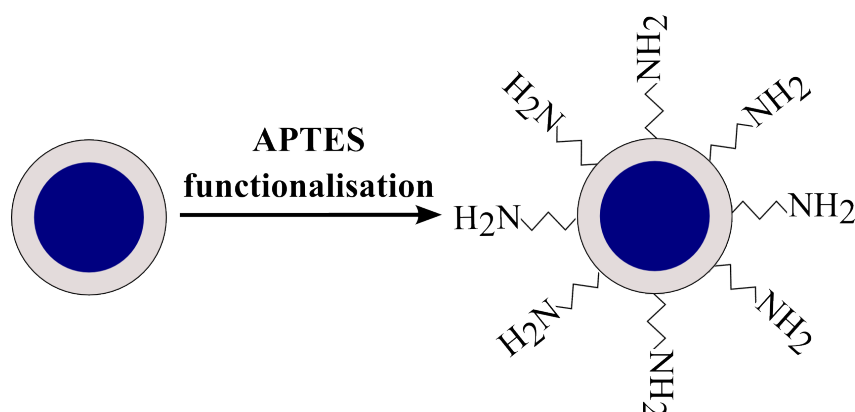


Figure 5.1: Overview of the reaction: the silica coated gold nanoparticles are functionalised with (3-aminopropyl)triethoxysilane. After functionalisation -NH_2 groups are present at the surface.

Surface functionalisation was performed based on work presented by C. Graf et al. [18]. According to this paper, the surface occupied by one (3-aminopropyl)triethoxysilane molecule equals 0.6 nm^2 . Furthermore, it is shown that 2.5 monolayers of organosilane is enough to functionalise the surface. For functionalisation enough material is provided to cover the particles with 2.5 monolayers of (3-aminopropyl)triethoxysilane.

Absorption spectra of the silica coated gold nanoparticles were used to estimate the particle concentration (see appendix C). The total particle diameter was determined by TEM measurements and these numbers were used to calculate the total surface of silica present per volume of gold nanoparticle solution.

In a typical functionalisation reaction, 1 mL gold nanoparticle solution and 1 mL ethanol were transferred to a vial and sonicated for 15 minutes. After sonication the right amount of a diluted (3-Aminopropyl)triethoxysilane solution was added to provide enough molecules to coat all gold nanoparticles with 2.5 monolayers of organosilane. Samples were sonicated for 3 hours and washed by centrifugation to remove any unbound (3-Aminopropyl)triethoxysilane. Finally particles were resuspended in 1 mL ethanol.

TEM measurements were used to ensure that the particles did not cluster during the process.

Chapter 6

Dye attachment and gold-dye coupling

In the final step of the reaction, the ATTO700 dye is bound to the -NH_2 functionalised silica surface of the silica coated gold nanoparticles as depicted schematically in figure 6.1. This bonding should be really easy since the activated ATTO700 dye is used in this step which enables bond formation between the dye and the -NH_2 groups at the surface.

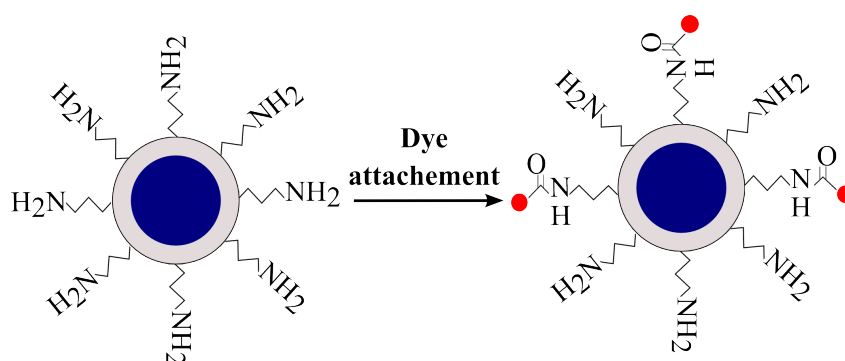


Figure 6.1: Overview of the reaction: the ATTO700 dye (red dots) is bound to the -NH_2 functionalised silica surface via the formation of a stable amide bond.

After dye binding, photoluminescence decay measurements were performed to investigate whether there is coupling between the gold nanoparticles and the dye at the surface. Also some theoretical calculations are included in this chapter, showing that for the gold nanoparticles it should be possible to observe enhancement of the dye emission.

6.1 Gold-dye coupling: theoretical calculations

A Mathematica script was written by Freddy Rabouw based on the model presented by Reineck et al. [8]. This script was used to perform all theoretical calculations included in this chapter. Calculations were performed for the ATTO700 dye. The maximum in absorption (λ_{abs}) is at 700 nm for this dye and the maximum in emission (λ_{fl}) is at 719 nm as stated by the supplier (see Appendix B).

In the first calculations the relative fluorescence intensity and lifetime of the dye was calculated as a function of the gold radius for a constant gold-dye separation, d , of 10 nm. Results of these calculations are included in figure 6.2. We can see from the figure that at this separation quenching is observed for small gold whereas enhancement is observed for gold nanoparticles with a radius over 43 nm. It would be really interesting to demonstrate this enhancement of the dye emission experimentally. From the graph showing the relative fluorescence lifetime it can be seen that for all gold sizes a shortening in the lifetime is expected.

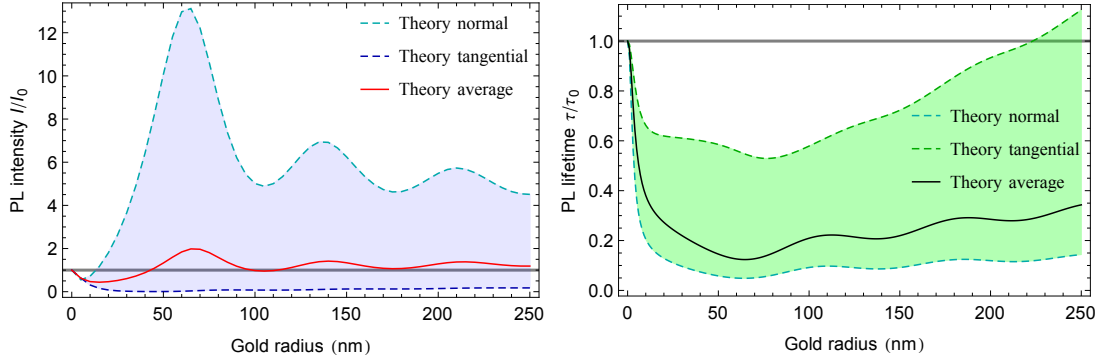


Figure 6.2: In (a) the theoretical results for the relative fluorescence intensity and in (b) for the relative fluorescence lifetime as a function of the gold radius calculated for a gold-dye separation, d , of 10 nm for the ATTO700 dye. Values are calculated for normal and tangential dye orientations (dashed lines) and were averaged to obtain the theory average (solid line).

If we now calculate the relative fluorescence intensity and lifetime as a function of the gold-dye separation for gold with a diameter of 55 nm (the radius equals 27.5 nm) we obtain plots included in figure 6.3. It can be seen that we expect to see enhancement of dye emission when the gold-dye separation, d , becomes larger than 16.5 nm. We can also see that for a separation of 10 nm we expect to see quenching of the dye-emission which is in agreement with the data presented in figure 6.2. Again we observe a shortening of the fluorescence lifetime for all separations. At small values of d , this effect is the strongest whereas this effects becomes smaller with increasing values of d .

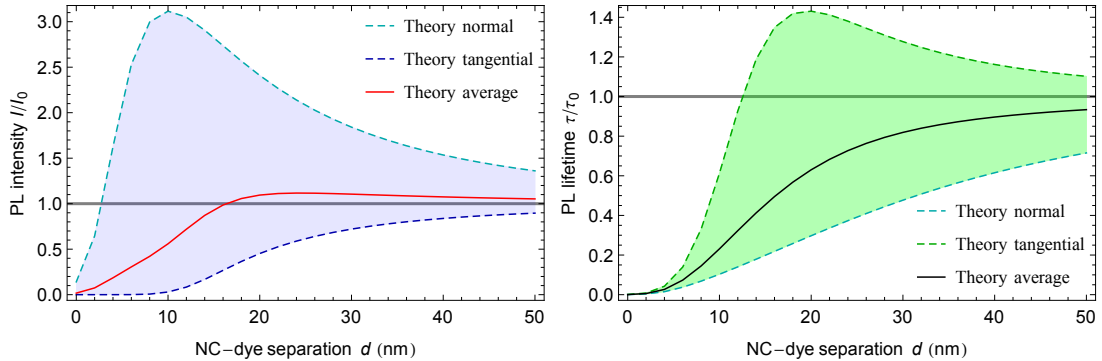


Figure 6.3: In (a) the theoretical results for the relative fluorescence intensity and in (b) for the relative fluorescence lifetime as function of the gold-dye separation, d , calculated for gold with a diameter of 55 nm (radius = 27.5 nm) for the ATTO700 dye. Values are calculated for normal and tangential dye orientations (dashed lines) and were averaged to obtain the theory average (solid line).

6.1.1 Atto700 stock solution - Absorption measurements

A stock-solution of ATTO700 in DMSO was prepared by dissolution of 1 mg ATTO700-NHS ester (as ordered) in 1 mL DMSO (anhydrous). For more information about the dye used in the experiments, see appendix B. Dissolution and storage of the dye was performed in absence of water and oxygen. Anhydrous DMSO was used because of limited the stability of the NHS-ester against hydrolysis. In order to be able to determine the exact concentration of the stock solution 3 mL ethanol and 10 μL of the stock solution was transferred to a cuvet and the absorption spectrum depicted in figure 6.4 was measured.

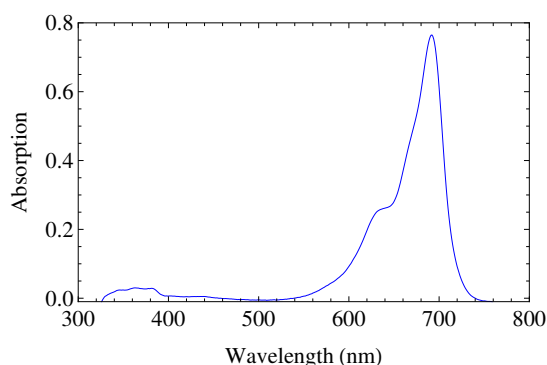


Figure 6.4: Absorption spectrum measured for the ATTO700 dye in ethanol.

A maximum in the absorption spectrum of 0.76479 was found at 692 nm. This maximum and the ϵ_{max} of $1.2 \cdot 10^5 \text{ M}^{-1}\text{cm}^{-1}$ (see Appendix B) were used to calculate the dye concentration in the diluted solution. After correcting for the dilution, a dye concentration of 1.92 mol L^{-1} for the DMSO stock solution was calculated.

6.2 Dye binding 1

For this experiment gold nanoparticles with an average diameter of 52 nm coated with an APTES functionalised silica shell with an average thickness of 13 nm were used. TEM pictures and an absorption spectrum of the particles are shown in figure 6.5. A gold nanoparticle concentration of $5.69 \cdot 10^{-11} \text{ mol L}^{-1}$ was calculated from the absorption spectrum.

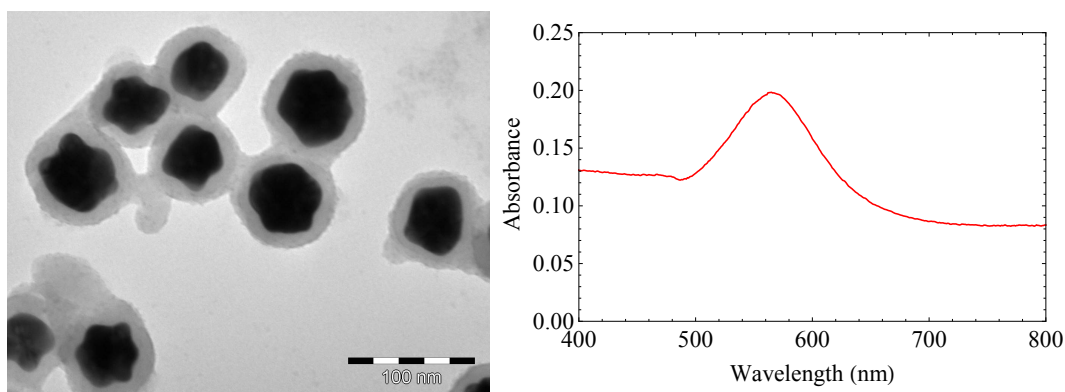


Figure 6.5: TEM picture (left) and absorption spectrum (right) of silica coated gold nanoparticles functionalised with APTES before dye binding.

For dye binding the ATTO700 stock solution was diluted in ethanol to obtain a 6 μM and a 3 nM solution.

200 μL of gold nanoparticle solution was transferred to two vials which were sonicated for 15 minutes. To one of the samples 18 μL of the 3 nM dye solution was added, to the other sample 18 μL of the 6 μM dye solution was added. After 3 hours of sonication 1 mL ethanol was added to both samples. Since the vials were in a horizontal position during sonication a lot of the gold was found inside the cap indicated by coloration of the rubber.

6.2.1 TEM measurements

In figure 6.6 TEM pictures recorded for the second sample are depicted, for this sample an excess of dye was added to the gold nanoparticles. From the pictures it can be seen that the particles tend to cluster to form big balls, this clustering into big balls was also observed for other samples in which an excess of dye was used.

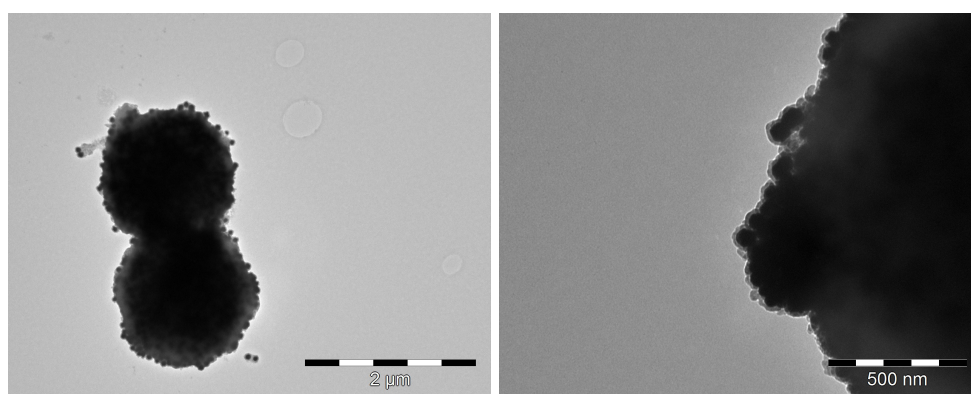


Figure 6.6: Clusters of silica coated gold nanoparticles are found after dye functionalisation with 18 μL 6 μM dye solution.

6.3 Dye binding 2

For this experiment gold nanoparticles with an average diameter of 55 nm coated with an APTES functionalised silica shell with an average thickness of 30 nm were used. TEM pictures and an absorption spectrum of the particles are shown in figure 6.7. A gold nanoparticle concentration of $1.35 \cdot 10^{-11} \text{ mol L}^{-1}$ was calculated from the absorption spectrum.

For dye binding the ATTO700 stock solution was diluted 1000 times in ethanol by transferring 10 mL ethanol and 10 μL of the ATTO700 stock solution in DMSO to a vial. 200 μL of gold nanoparticle solution was transferred to a vial and sonicated for 15 minutes. 5 μL of the 1000 times diluted ATTO700 solution was added under sonication. After 3 hours of sonication 1 mL ethanol was added and samples were stored.

1 extra mL ethanol was added and the sample was transferred to a cuvet. An emission spectrum was recorded exciting the sample at 650 nm. The sample was transferred to a vial and centrifuged 30 min at 3500 rpm. As much supernatant as possible was removed and transferred to a different vial. 1 mL ethanol was added to the supernatant and the precipitate. Dissolution of the precipitate was ensured by sonication.

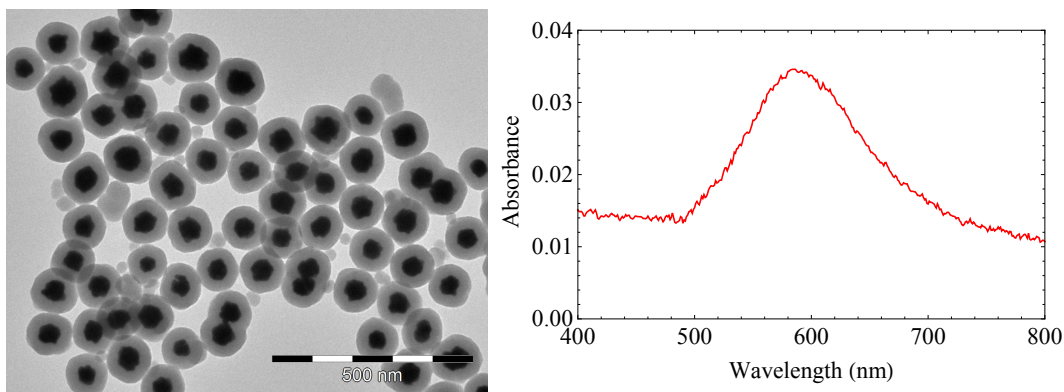


Figure 6.7: TEM picture (left) and absorption spectrum (right) of silica coated gold nanoparticles functionalised with APTES before dye binding.

6.3.1 Emission measurements

Emission measurements were performed before and after centrifugation for the supernatant as well as the precipitate and are included in figure 6.8 after excitation at 650 nm.

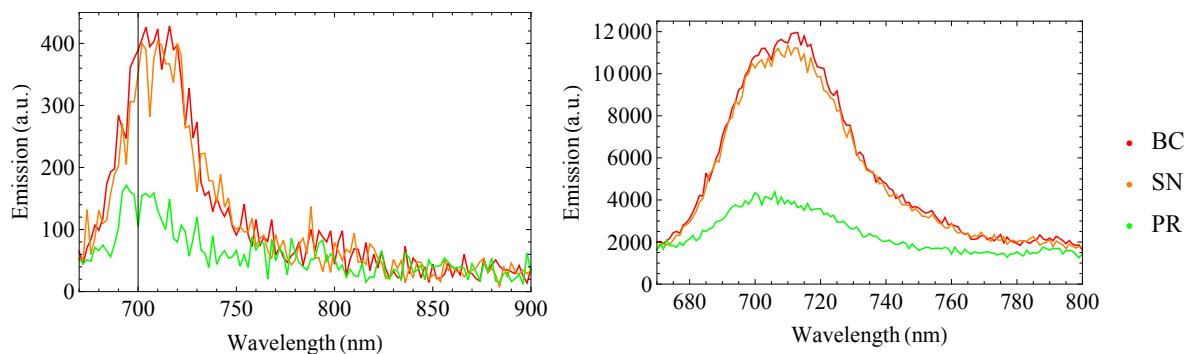


Figure 6.8: Emission spectra after dye binding before centrifugation (BC) and after centrifugation for the supernatant (SN) and the precipitate (PR). Samples were excited at 650 nm.

A peak around 710 nm is observed in all samples indicating the presence of the ATTO700 dye. Before centrifugation the presence of the dye is expected. However, dye emission is also observed in the supernatant as well as the precipitate. The emission observed in the supernatant indicates the presence of unbound dye molecules that are removed from the gold nanoparticles during the centrifugation step.

The intensity of the dye emission in the precipitate is much lower compared to the other two samples. This indicates that also the dye emission is much lower in this sample. This can be explained in two ways. The first explanation is that not all dye molecules were removed by centrifugation. This is a plausible explanation since it was not possible to remove all liquid after centrifugation. The second explanation is that some dye molecules are attached to the gold nanoparticles. From this results only it is impossible to determine whether dye binding was successful.

6.4 Dye binding 3

Gold nanoparticles with an average diameter of 55 nm coated with an APTES functionalised silica shell with an average thickness of 18 nm were used. TEM pictures and an absorption spectrum of the particles are shown in figure 6.9. A gold nanoparticle concentration of $6.98 \cdot 10^{-11}$ mol L⁻¹ was calculated from the absorption spectrum.

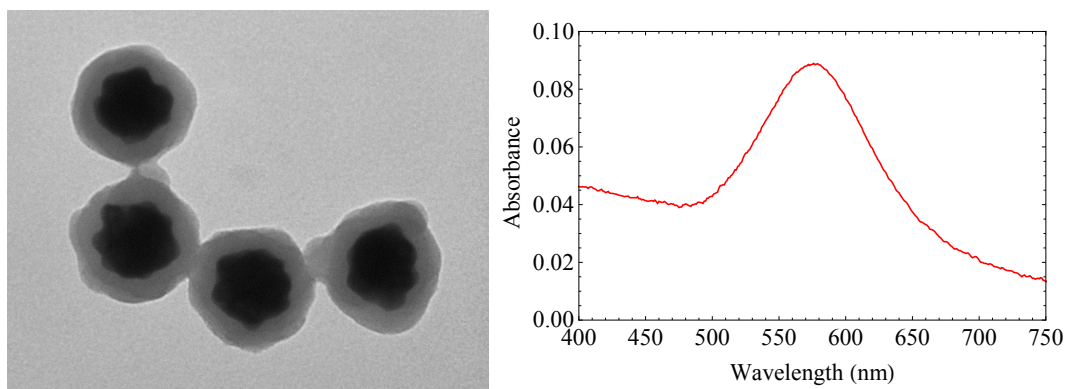


Figure 6.9: TEM picture (left) and absorption spectrum (right) of silica coated gold nanoparticles functionalised with APTES before dye binding.

For dye binding, 250 μ L of gold nanoparticle solution was transferred to two separate vials (a) and (b). To the first vial, 5 μ L of the 1000 times diluted ATTO stock solution was added. To the second vial 5 μ L of the 10.000 times diluted stock solution was added. After 3 hours of sonication, 3 mL ethanol was added to both samples. Two reference solutions containing the same dye concentrations were prepared by transferring 5 μ L 1000 and 10.000 times diluted ATTO700 stock solution and 3250 μ L ethanol to two separate vials.

6.4.1 Emission measurements

Photoluminescence decay measurements were performed 700 nm for all 4 samples after excitation with a pulsed laser at 656.6 nm and are included in figure 6.10. A bi-exponential fitting procedure was used to fit the data according to the following formula:

$$N(t) = a \exp(-t/\tau_1) + b \exp(-t/\tau_2) + c \quad (6.1)$$

In this formula t corresponds to the time after the laser pulse, τ_1 and τ_2 correspond to the fluorescence lifetimes of the two decay processes and a , b and c are constants.

From figures (a) and (b) we can conclude that only one single-exponential decay path is available for dye emission in the absence of gold (blue dots). We can also see that a second much faster decay path appears when in the presence of the gold particles (red dots). We can conclude from this that the second, faster, decay path is caused by the presence of gold. This indicates that there is coupling between the gold particles and dye molecules.

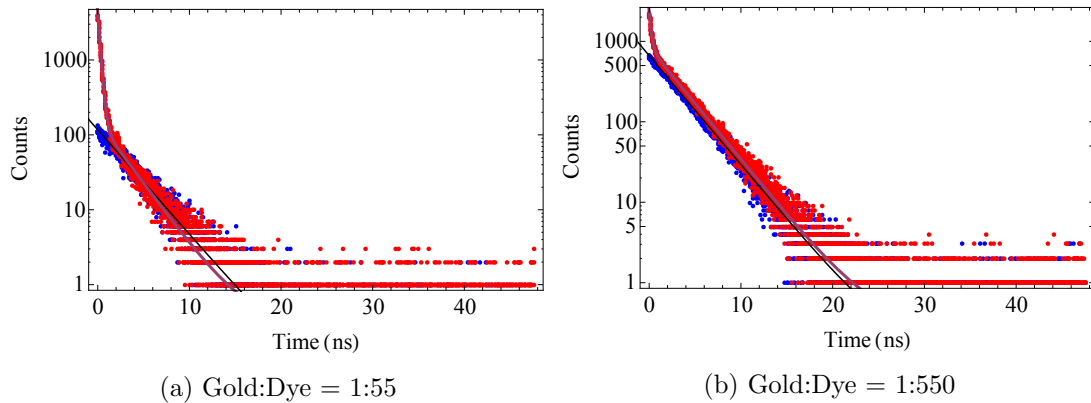


Figure 6.10: Photoluminescence decay measurements recorded at 700 nm after pulsed excitation at 656.6 nm. The blue dots correspond to dye solution containing no gold particles, the red dots correspond to solutions containing the same concentration of dye after gold-dye binding. The gold:dye ratio is increased by a factor of 10 going from (a) to (b) whereas the gold nanoparticle concentration remains the same. The solid lines were fitted to the data assuming a bi-exponential decay process.

In figure (a) this feature is more pronounced than in (b). This can be explained by the difference in concentration of the dye molecules between samples (a) and (b). For gold-dye coupling to appear, the dye molecules have to be very close or attached to the gold particles. In sample (b) the dye concentration is increased by a factor of 10 compared to the concentration of gold, which is the same in both samples. Because of this increase in dye concentration relatively more signal is collected from dyes that do not couple to the gold particles, i.e. gold particles that are at a distance of the gold particles to large for coupling to occur. An explanation would be that the surface of the silica coated gold particles becomes saturated at low dye concentrations. If the dye concentration is increased after saturation of the surface, no more dyes attach to the surface so the amount of dye molecules coupling to the gold particles remains the same.

In table 6.1 lifetimes calculated for the four solution are listed. Here τ_1 corresponds to the lifetimes of the dye in the absence of gold whereas τ_2 corresponds to the lifetime of the dyes that are coupling to the gold particles. We can again conclude that there is coupling in the presence of gold since a faster decay path appears in the presence of the gold particles.

Sample	τ_1 (ns)	τ_2 (ns)	fraction gold-dye signal
Atto (2)	3.11	-	
Gold-dye (a)	2.63	0.25	0.73
Atto (1)	3.20	-	
Gold-dye (b)	3.12	0.23	0.12

Table 6.1: τ_1 , τ_2 and fraction.

The fraction of signal collected from dyes that do couple to the gold particles is calculated according to the following formula:

$$\text{Fraction}_{\text{gold-dye}} = \frac{b\tau_2}{a\tau_1 + b\tau_2} \quad (6.2)$$

A fraction of 0.73 is found for sample (a), a fraction of 0.12 is found for sample (b). Both values are included in table 6.1 and agree with earlier observations that more unbound dye is present in sample (b). This makes it reasonable to conclude that dye binding has been successful and that the gold particles and dye molecules do couple.

A shortening of the lifetime was expected for these gold nanoparticles. However, it is not possible to determine whether the observed lifetime agrees with the predicted value since we do not know τ_0 . To determine τ_0 we have to determine the lifetime of the dye attached to a silica sphere in the absence of gold. It is also not possible to determine whether this coupling results in quenching or enhancement of dye emission. To distinguish between the two processes, we have to measure I and I_0 . I corresponds to the intensity of the dye emission when the dye is attached to the silica coated gold particles. I_0 corresponds to the intensity of dye emission when the dye is attached to silica spheres in the absence of gold.

Chapter 7

Conclusion

Gold nanoparticles with diameters ranging from 50 to 200 nm were synthesized successfully in a two step synthesis. In the first step, gold seeds with diameter close to 16 nm were prepared via a citrate reduction. In the second step, hydroquinone was used as a reductor to deposit gold ions selectively onto the seeds. It was demonstrated that it is possible to tune the final size of the particles by changing the number of seeds added in the second step. Absorption and TEM measurements were used to characterize the particles that were obtained. It was observed that the absorption of the gold nanoparticles shifts to longer wavelengths with increasing sizes. Also peak broadening and an increase in the amount of scattering was observed for bigger particles which is in agreement with theory.

The obtained particles were coated with PVP and transferred to ethanol. Via an adjusted Stöber process it was possible to grow a silica shell around the gold nanoparticles. During this process, ammonia was added to the gold nanoparticle solution in ethanol and small portions of tetraethylorthosilicate were added over time. TEM measurements show that during this addition shells are formed. However, also a lot of secondary nucleation of silica was observed. The amount of secondary nucleation could be decreased by decreasing the amount of PVP added for stabilisation of the particles. After decreasing this amount, it was possible to grow silica shells and control over the shell thickness was obtained.

The outer surface of the particles was functionalised with (3-aminopropyl)triethoxysilane introducing $-NH_2$ groups. These groups were used to bind the activated ATTO700 dye to the surface. After dye binding, photoluminescence decay measurements were used to determine whether there was coupling between the gold nanoparticles and the dyes at the surface. This coupling was indeed observed for gold with a diameter of 55 nm and a silica shell with a thickness of 18 nm. Coupling was indicated by the presence of a second, much faster decay path for dye emission that was not observed in the absence of the gold nanoparticles. In the absence of the gold nanoparticles, only one decay path was observed. It is also observed that the fraction of dye emission coupling to the gold increases with a decreasing gold-dye ratio since the faster decay path is observed more pronounced compared to the normal decay path for a lower gold-dye ratio.

Besides the experimental work theoretical calculations were performed showing that for bigger gold nanoparticles (typically > 50 nm in diameter) also enhancement of dye emission is possible. This is in contrast to the study performed by Reineck et al. [8] for gold nanoparticles with a diameter of 12.7 nm. For these particles only quenching of dye emission is expected because of the small size of the particles and this is also what was observed.

Despite the observed gold-dye coupling it is not possible to conclude anything more about this coupling than that it does take place. In order to learn more about this coupling a comprehensive study is necessary. It would be for example interesting to study the dependence of the dye emission on the separation between the gold nanoparticle and the dye for different sizes of gold. This was the ultimate goal of this work but because of limited time and the time to develop a procedure for the sample preparation, this was not achieved. However, it should be achievable to do these measurements since a reproducible way to synthesise the samples necessary for this study is presented.

Chapter 8

Outlook

Based on the results obtained in this thesis, ideas for further research will be summarized below.

- A comprehensive study of the gold-dye coupling is necessary to determine whether the theoretical model presented by Reineck et al. is also applicable for bigger gold nanoparticles. By following the procedures presented in this thesis it is possible to synthesize samples to study how gold-dye coupling depends on the separation between the gold nanoparticles and the dye for different sizes of gold nanoparticles.
- Silica spheres with different sizes can be synthesized according to the Stöber procedure. After functionalisation with (3-aminopropyl) triethoxysilane, dyes can be attached to the surface of these spheres. Measurements on these samples can be used as a reference for the measurements performed for the silica coated gold nanoparticles (τ_0 and I_0).
- It would be interesting to study coupling between gold nanoparticles and quantum dots, for example the core multishell quantum dots presented in part B of this thesis. If a stable dispersion of the multishell quantum in ethanol can be obtained, it might be possible to bind the particles to the $-NH_2$ functionalised, silica coated gold nanoparticles. After binding it should be possible to study coupling between the quantum dots and the gold nanoparticles. Stabilisation of the quantum dots in ethanol can be achieved for example by coating the particles with 11-mercaptoundecanoic acid [19].

Acknowledgments

The results I have presented in this report would not have been accomplished without the help of many people and therefore I would like to thank them here.

At first I would like to thank my daily supervisors, Freddy and Relinde. I had the luxury of having two daily supervisors which was great. Freddy, thanks for all your help and patience when I was struggling with Mathematica or theory needed for this thesis. You have provided me with most of the scripts I needed to do the calculations included in this thesis. Furthermore, you have provided me with the knowledge and theory to understand these calculations since most of the concepts were new for me. Relinde, thanks for helping me with the synthesis part of this thesis. You have been a great support in and around the lab. It really felt like I could ask you everything concerning chemical syntheses. I also really enjoyed all TEM sessions and coffee breaks we have had so far. We have had a lot of valuable discussions which made me reconsider my own procedures and helped me continuing my work at the lab.

Professor Vanmaekelbergh, I would also like to thank you as my supervisor. Your enthusiasm about my results really kept me going during this project. Besides, I truly appreciate your help with finding a PhD position, an exciting next step in my career in research.

Furthermore, I would like to thank all other members and students of Condensed Matter & Interfaces that I have met during this project. I have learned a lot from all of you during my time at CMI and all group meetings and discussions we have had were really valuable. I also really enjoyed my time at CMI and I am really grateful for this. All coffee breaks, lunches, borrels, Christmas dinners and uitjes were great and you have all contributed to that!

I would like to end with thanking my friends and family who have been really supporting, understanding and encouraging, throughout my whole study. I want to thank everyone for putting in the effort to truly understand the topics on which I have been working since the "nanoworld" was new for most of you. My special thanks go to my beloved parents, brother and sister for all the help and support they gave me when I was confused or really busy.

I would like to thank my dear friends at the zogro, Rowanne, Bianca and Wynneke. I really appreciate all the nice sunday evening talks and dinner dates we have had and I am really proud of everything we have achieved so far. Josine, I am thanking you not only as a fellow student but also as a good friend. Thanks for all the (chemistry related) discussions we have had in Utrecht and after I went to Amsterdam for my internship.

I would like to conclude with thanking everyone I did not mention personally in here since I know there are many others to thank.

Bibliography

- [1] Ulf Leonhardt, “Invisibility cup,” *Nature photonics*, vol. 1, pp. 207–208, April 2007.
- [2] Kenneth Chang, “Tiny Is Beautiful: Translating ‘Nano’ Into Practical,” *The Newyork Times*, 2005.
- [3] Marie-Christine Daniel and Didier Astruc, “Gold Nanoparticles: Assembly, Supramolecular Chemistry, Quantum-Size-Related Properties, and Applications toward Biology, Catalysis, and Nanotechnology,” *Chemical Reviews*, vol. 104, pp. 293–346, 2004.
- [4] H. Mertens, A.F. Koenderink and A. Polman, “Plasmon-enhanced luminescence near noble-metal nanospheres: Comparison of exact theory and an improved Gerstend and Nitzan model,” *Physical Review B*, vol. 76, pp. 115123 1–12, 2007.
- [5] Jiri Homola, Sinclair S. Yee, Guünter Gauglitz, “Surface plasmon resonance sensors: review,” *Sensor and Actuators B*, vol. 54, pp. 3–15, 1999.
- [6] Katherine A. Willets and Richard P. Van Duyne, “Localized Surface Plasmon Resonance Spectroscopy and Sensing,” *Annual Review of Physical Chemistry*, vol. 58, pp. 267–297, 2007.
- [7] Xiaohua Huang, Pashant K. Jain, Ivan H. El-Sayed and Mostafa A. El-Sayed, “Gold nanoparticles: interesting optical properties and recent applications in cancer diagnostics and therapy,” *Nanomedicine*, vol. 2, pp. 681–693, 2007.
- [8] Philipp Reineck, Daniel Gómez, Soon Hock Ng, Matthias Karg, Toby Bell, Paul Mulvaney and Udo Bach, “Distance and Wavelength Dependent Quenching of Molecular Fluorescence by Au/SiO₂ Core-Shell Nanoparticles,” *ACS Nano*, vol. 7, pp. 6636–6648, 2013.
- [9] W. Stöber and A. Fink, “Controlled Growth of Monodisperse Silica Spheres in the Micron Size Range,” *Journal of colloid and interface science*, vol. 26, pp. 62–69, 1968.
- [10] Herbert Giesche, “Synthesis of Monodispersed Silica Powders II. Controlled Growth Reaction and Continuous Production Process,” *Journal of the European Ceramic Society*, vol. 14, pp. 205–214, 1994.
- [11] Kan-Sen Chou and Chen-Chih Chen, “The critical conditions for secondary nucleation of silica colloids in a batch Stöber growth process,” *Ceramics International*, vol. 34, pp. 1623–1627, 2008.
- [12] Ping Yang, Kazunori Kawasaki, Masanori Ando, Norio Murase, “Au/SiO₂/QD core/shell/shell nanostructures with plasmonic enhanced photoluminescence,” *Journal of Nanoparticle Research*, vol. 14, pp. 1–11, 2012.

- [13] Yu Lu, Yadong Yin, Zhi-Yuan Li and Younan Xia, "Synthesis and Self-Assembly of AuSiO₂ Core-Shell Colloids," *Nano Letters*, vol. 2, No. 7, pp. 785–788, 2002.
- [14] Eiichi Mine, Akira Yamada, Yoshio Kobayashi, Mikio Konno and Luis M. Liz-Marzán, "Direct coating of gold nanoparticles with silica by a seeded polymerization technique," *Journal of Colloid and Interface Science*, vol. 264, pp. 385–390, 2003.
- [15] C. Graf, D.L.J. Vossen, A. Imhof and A. van Blaaderen, "A General Method To Coat Colloidal Particles with Silica," *Langmuir*, vol. 19, pp. 6693–6700, 2003.
- [16] Steven D. Perrault and Warren C.W. Chan, "Synthesis and Surface Modification of Highly Monodispersed, Spherical Gold Nanoparticles of 50-200 nm," *Journal of the American Chemical Society*, vol. 131, pp. 17042–17043, 2009.
- [17] Nano Composit Europe, "Gold Nanoparticles: Optical Properties." <http://nanocomposix.eu/pages/gold-nanoparticles-optical-properties>. [Online; accessed 8-8-2014].
- [18] Christina Graf and Alfons van Blaaderen, "Metallo-dielectric Colloidal Core-Shell Particles for Photonic Applications," *Langmuir*, vol. 18, pp. 524–534, 2002.
- [19] J. Immink, "Synthesizing and Characterizing CdS/PbS/Cd(OH)₂ Quantum Dots."
- [20] Douglas Hayworth-Thermo Scientific, "Amine-reactive Crosslinker Chemistry." <http://www.piercenet.com/method/amine-reactive-crosslinker-chemistry>. [Online; accessed 8-8-2014].
- [21] P.B. Johnson and R.W. Christy, "Optical Constants of the Noble Metals," *Physical Review B*, vol. 6, number 12, pp. 4370–4379, 1972.

Appendices

A: Chemicals

Chemical	Manufacturer	Purity	M_w g mol ⁻¹
tri-Sodium citrate dihydrate	Merck	pro analysi	294.10
Gold(III) chloride hydrate / Chloroauric acid	Sigma Aldrich	99.999% trace metals basis	393.83
Hydroquinone	Alfa Aesar	98.5 %	110.11
Polyvinylpyrrolidone - PVP10	Sigma Aldrich	-	10 000
Tetraethylorthosilicaat (TEOS)	Sigma Aldrich	99.999% trace metals basis	208.33
(3-Aminopropyl)triethoxysilane	Sigma Aldrich	99%	221.37
Ethanol	Alfa Aesar	Anhydrous, 94 - 96%	46.07
Ammonium hydroxide	Sigma Aldrich	28% ammonia in water, 99.99+%	35.05
Sodium hydroxide	Merck	pro analysi	40.00
Tetrakis(hydroxymethyl) - phosphonium chloride	Sigma Aldrich	80% solution in water	190.56
Dimethyl sulfoxide - DMSO	Sigma Aldrich	Anhydrous, 99.9%	78.13

B: ATTO700 dye

For the experiment, the ATTO700 dye purchased at ATTO-TEC GmbH in Germany was used. In figure 8.1 emission and fluorescence spectra of the ATTO700 dye are shown. Table 8.1 contains optical data of the carboxy derivate[20].

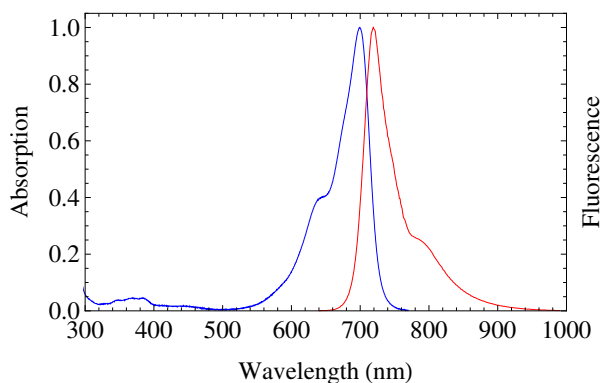


Figure 8.1: Absorption spectra (blue) and fluorescence spectra (red) of the ATTO700 dye.

λ_{abs}	700 nm
ϵ_{max}	$1.2 \times 10^5 \text{ M}^{-1}\text{cm}^{-1}$
λ_{fl}	719 nm
η_{fl}	25%
τ_{fl}	1.2 ns
CF ₂₆₀	0.26
CF ₂₈₀	0.41

Table 8.1: Optical data of the ATTO700 carboxy derivate of in water

To be able to couple the dye to the APTES functionalised silica layer around the gold nanoparticles, the NHS ester of the dye is used. For this compound, the carboxylic acid of the dye is activated by the formation of an esterbond with N-Hydroxysuccinimide. This ester easily reacts with amino-groups according to the reaction scheme depicted in figure 8.2 to form a stable amide bond.

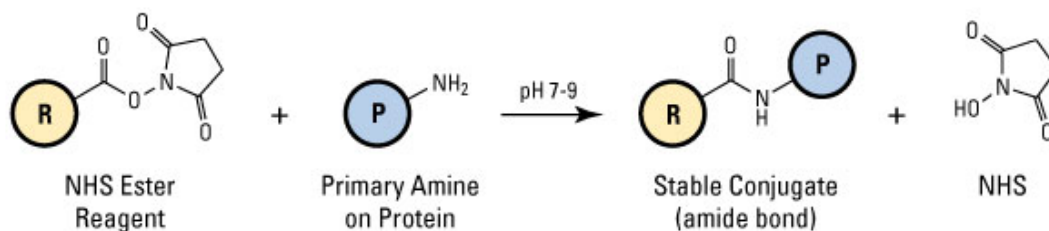


Figure 8.2: Coupling of an -NHS activated carboxylic acid to a primary amine.

C: Calculation of extinction for spherical gold nanoparticles

A script written by Freddy Rabouw was used to calculate the extinction of spherical gold nanoparticles at different wavelengths. The Drude Model was assumed to be valid and the optical data for gold presented by Johnson et al. [21] was used. In figure 8.3 the extinction is plotted as a function of the wavelength for gold with radii from 1 to 60 nm. Peak broadening and a shift of the maximum extinction to longer wavelengths is clearly observed with increasing gold radius.

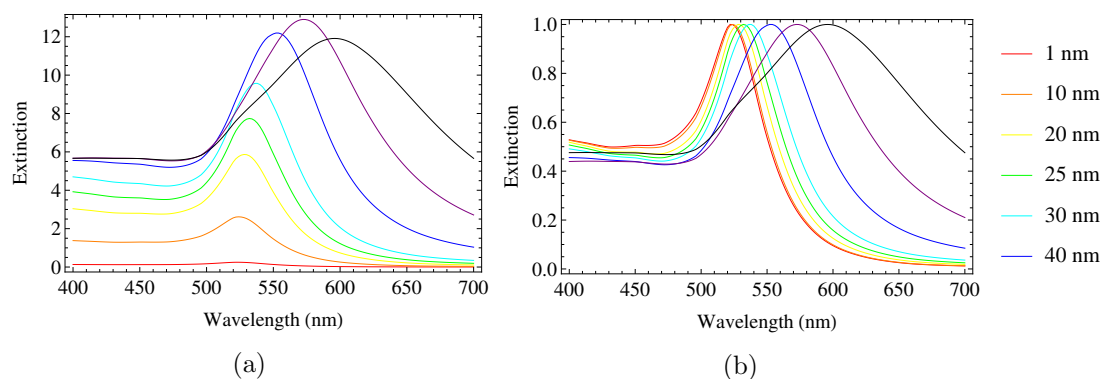


Figure 8.3: In (a) the extinction and in (b) the normalised extinction is plotted as a function of the wavelength calculated for spherical gold nanoparticles with different radii.

Comparison with the absorption spectra measured for the gold rainbow

The absorption spectra for 5 different sizes of gold nanoparticles are included in figure 8.4 (see section 3.2) indicated by the solid lines. Here the diameters of the gold nanoparticles were determined from TEM measurements. These diameters were used to calculate extinction spectra and are indicated by the dotted lines.

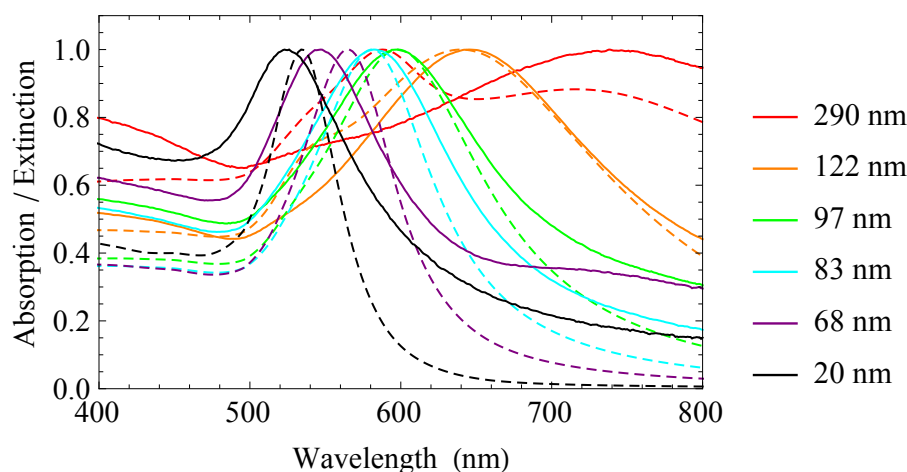


Figure 8.4: Solid lines correspond to normalised absorption spectra measured for different gold sizes where the average particle diameter is included in the legend. Dotted lines correspond to the calculated extinction spectra.

It can be seen that good agreement in peak position is observed for samples with diameters of 122 (orange), 97 (green) and 83 (cyan) nm. For the samples with 68 (purple) and 20 (black) nm the peaks that were calculated are found at longer wavelengths than is predicted by the measurements. Furthermore for the 290 nm sample (red) a second peak around 600 nm is observed in the calculations. This peak is not observed in the measurements. This can be caused by the underestimating of scattering in the calculations.

For all calculations included in this thesis an extinction coefficient of 15.12 was used. This value corresponds to the average value calculated for gold with a diameter of 50, 52, 71 or 113 nm in diameter.